E4.55 SOLUTIONS 2017

Question 1 Answer

a)

A: *n*+ source and drain regions of the *n*-channel MOSFET.
B: *p*+ source and drain regions of the *p*-channel MOSFET.
C: *n*-well, for the fabrication of the *p*-channel MOSFET.
D: Gate, fabricated using metal or heavily-doped polysilicon

1 mark each.

[4]

b)

$$|2S\rangle = \psi_{200} \sim \left(1 - \frac{zr}{2a_0}\right) e^{-2r/2a_0}$$

$$|2p_0\rangle = \psi_{210} \sim e^{-2r/2a_0} \cdot r\cos\theta$$

$$|2p_{\pm1}\rangle = \psi_{21,\pm1} \sim e^{-2r/2a_0} \cdot e^{\pm i\phi} r\sin\theta$$

The $|2p\rangle$ states can be rewritten as (see diagram):

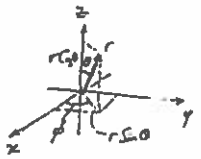

$$|2p_z\rangle = \psi_{210} \sim r\cos\theta\, e^{-2r/2a_0}$$

$$= z\, e^{-2r/2a_0}$$

[2]

and

$$|2p_{\pm1}\rangle = \psi_{21,\pm1} = e^{-2r/2a_0} e^{\pm i\phi} r\sin\theta$$

$$= e^{-2r/2a_0} (r\sin\theta)(\cos\phi \pm i\sin\phi)$$

$$= e^{-2r/2a_0} (x \pm iy)$$

[2]

We may then construct the linear combinations:

$$|2p_x\rangle = \frac{\psi_{21,1} + \psi_{21,-1}}{2} = x e^{-2r/2a_0}$$

$$|2p_y\rangle = \frac{\psi_{21,1} - \psi_{21,-1}}{2i} = y e^{-2r/2a_0}$$

[2]

These states are sketched below:

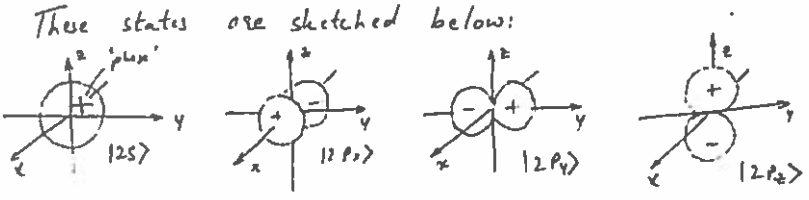

[2]

c) The unit cell in a Si lattice, with side length a, is shown below:

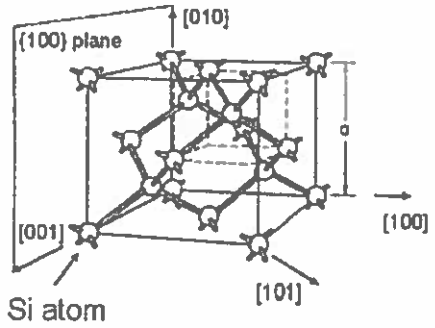

This may be constructed by interleaving two FCC cells, displaced by $a/4$ along the x, y and z axis, as follows:

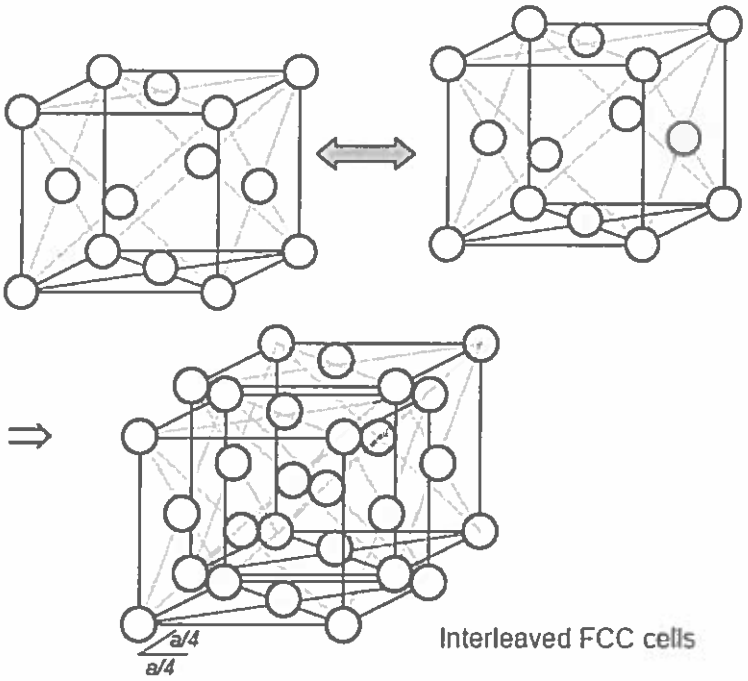

Dropping atoms outside the unit cell gives us the Si unit cell:

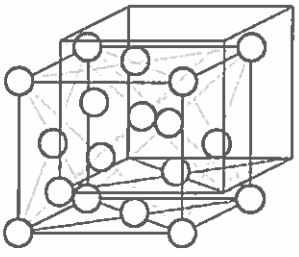

[4]

d) Resonant tunnelling diodes typically use double-barrier heterostructures to form a potential well along one dimension. For example, in a n^+GaAs/AlAs/i-GaAs/AlAs/n^+GaAs heterostructure, the AlAs layers form tunnel barriers and the central GaAs region forms a potential well. A simplified band diagram is shown below:

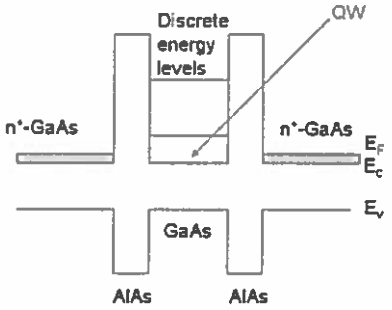

The discrete states in the well lead to current peaks in the I-V characteristics, as they drop below the conduction band edge in the source. Current flows when a state overlaps with filled states in the source. The process is shown below diagrammatically, for a single current peak/state in the well:

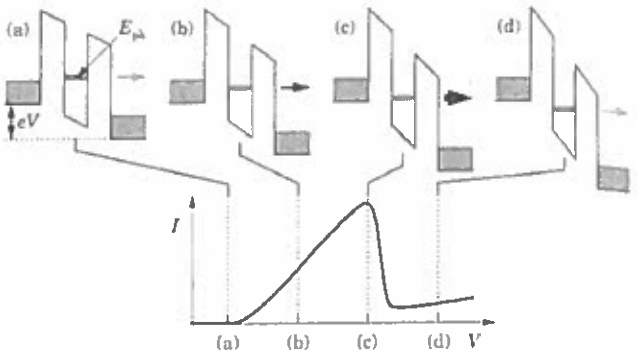

[4]

e) Using the method of sections, the bending moment is given by:

$$M(x) = p(L-x)\cdot\frac{(L-x)}{2}$$

where x is distance along the beam, and L is the beam length. The bending equation is therefore:

$$\frac{d^2v}{dx^2} = \frac{M}{EI} = p\frac{(L-x)^2}{2EI}$$

where E is Young's modulus and I is the second moment of area. Integrating twice, and applying the boundary conditions $v' = 0$, $v = 0$ at $x = 0$, gives:

$$v = \frac{p}{6EI}\left[L^3x + (L-x)^4/4 - L^4/4\right] \qquad [3]$$

The axial stress is given by $\sigma = -Eyv'' = -My/I$ where y is the distance from the neural axis. Substituting for M, this becomes:

$$\sigma = -Eyv'' = -\frac{py(L-x)^2}{2I}$$

Since $0 \le x \le L$, and $-h/2 \le y \le h/2$, where h is the depth of the beam in the direction of the applied load, the maximum tensile stress will be:

$$\sigma_{max} = \frac{|p|L^2h}{4I}. \qquad [2]$$

f) Bulk micromachining is based primarily on anisotropic etching. Certain alkaline etchants (for example EDP and KOH/IPA) attack silicon at very different rates in different crystallographic directions. Etching is fastest along <100> directions and slowest along <111> directions, with other crystal directions exhibiting intermediate rates. The ratio of <100> to <111> etch rates can be up to 400.

Anisotropic etching allows cavities to be produced in a silicon wafer where the bounding walls are defined by {111} crystal planes. In a (100)-oriented wafer these planes are at an angle of 54.7° to the wafer surface, so anisotropically etched cavities in a (100) wafer are tapered towards the bottom. In a (110)-oriented wafer there are {111} planes normal to the surface so vertical-walled cavities can be produced.

Bulk micromachining tends to be used to realise simple structures such as V-grooves, membranes (by removal of material from the back side of the wafer) and cavities. Cantilevers and built-in beams can also be produced by undercutting a surface layer. The etch rate along <100> can be relatively high, allowing large features to be produced in a reasonable time. [5]

g) If the resolution is limited by diffraction, then it will be given by $R \sim \lambda/NA$ where λ is the wavelength and NA is the numerical aperture. For an electron beam system, λ is the de Broglie wavelength and NA is half the convergence angle of the beam. For the system in question:

$\lambda = h/p = h/\sqrt{(2mE)} = 6.63e{-}34/\sqrt{(2 \times 9.1e{-}31 \times 5e4 \times 1.6e{-}19)} = 5.5$ pm
$NA = 5{\times}10^{-4}$
$\Rightarrow R \sim 11$ nm

In practice, the minimum achievable feature size in resist will be larger than this because of machine-related factors affecting the minimum spot size (finite source size and aberrations in the electron optics) and scattering in the resist and substrate. [5]

g) Electrothermal actuators use on differential thermal expansion between different parts of a structure to generate motion. In a material bimorph actuator, the differential thermal expansion occurs between two dissimilar materials that are in intimate contact, while in a shape bimorph actuator the device geometry leads to temperature differentials between different parts of a single mechanical layer. Heating is generally achieved by passing a current through either the mechanical layer or a deposited heater layer.

Material bimorph:

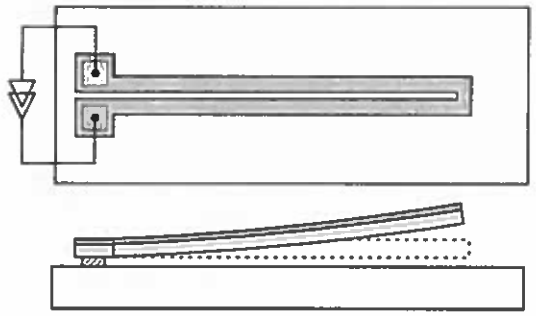

Shape bimorph:

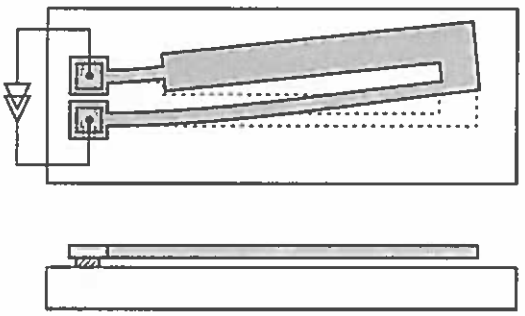

Material bimorph actuators generally produce out-of-plane motion, while shape bimorph generally produce in-plane motion. Shape bimorph actuators are easier to fabricate because they can be realised in a single layer. They are also less prone to unwanted deflections due to intrinsic stress and ambient temperature variations. [5]

Question 2 Answer

a) Charge neutrality over the entire nanowire ⇒

Charge trapped on the surface = charge lost from the interior of the nanowire. [2]

$\Rightarrow e.N_S.2\pi RL = eN_D.\pi(R^2 - r^2)$. [4]
$\Rightarrow N_S.2R = N_D\,(R^2 - r^2)$
$\Rightarrow (N_S/N_D)2R = R^2 - r^2$
⇒

$$r = \sqrt{R^2 - 2R\frac{N_S}{N_D}}$$

[4]

= 19.36 nm

b) Width of depleted region = $W = R - r$ = 25 nm - 19.36 nm = 5.64 nm

∴ surface potential

$$V_s = \frac{eN_D W^2}{2\varepsilon_r \varepsilon_0}$$

= 0.048 V

[4]

Band diagram along the nanowire diameter:

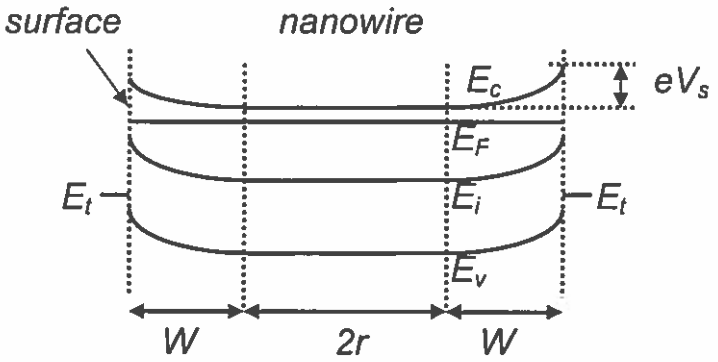

[4]

c) For 'Flat-band' voltage, we need the gate oxide capacitance per unit area, C_{ox}:

$C_{ox} = \varepsilon_{ox}\varepsilon_0 / t_{ox}$ = 2.3 milliF/m^2

[3]

For a surface charge density Q_s, 'Flat-band' voltage = $V_{FB} = -Q_s/C_{ox} = +eN_S/C_{ox}$
⇒ V_{FB} = +0.7 V

[3]

d) This is a depletion mode device. The threshold voltage V_{th} corresponds to the depletion across the entire nanowire, i.e. for depletion width $W = R$.

[2]

The threshold voltage is negative in value, as this is necessary to deplete an n-type nanowire. The threshold voltage is then given by:

$V_{th} = -|$voltage needed to fully deplete the nanowire – flat band voltage$|$
$= -(eN_D R/C_{ox} - V_{FB}) = -2.78$ V

[4]

Question 3 Answer

a) The boundary transmission matrices Γ_1 and Γ_2 are related to the electron wave function amplitudes as follows:

$$\begin{pmatrix} \alpha \\ \beta \end{pmatrix} = \frac{1}{2\,\mathrm{Re}[k]} \begin{pmatrix} k\exp\left(k^*\frac{a}{2}\right) & k^*\exp\left(k\frac{a}{2}\right) \\ k^*\exp\left(-k\frac{a}{2}\right) & k\exp\left(-k^*\frac{a}{2}\right) \end{pmatrix} \begin{pmatrix} A \\ B \end{pmatrix} = \Gamma_1 \begin{pmatrix} A \\ B \end{pmatrix}$$

$$\begin{pmatrix} C \\ D \end{pmatrix} = \frac{i}{2\,\mathrm{Im}[k]} \begin{pmatrix} -k\exp\left(k^*\frac{a}{2}\right) & k^*\exp\left(-k\frac{a}{2}\right) \\ k^*\exp\left(k\frac{a}{2}\right) & -k\exp\left(-k^*\frac{a}{2}\right) \end{pmatrix} \begin{pmatrix} \alpha \\ \beta \end{pmatrix} = \Gamma_2 \begin{pmatrix} \alpha \\ \beta \end{pmatrix}$$

[2]

We then have Γ_{single} as follows:

$$\begin{pmatrix} C \\ D \end{pmatrix} = \Gamma_2\Gamma_1 \begin{pmatrix} A \\ B \end{pmatrix} = \Gamma_{single} \begin{pmatrix} A \\ B \end{pmatrix} \Rightarrow$$

$$\Gamma_{single} = \frac{i}{2\,\mathrm{Im}[k]} \cdot \frac{1}{2\,\mathrm{Re}[k]} \begin{pmatrix} -k\exp\left(k^*\frac{a}{2}\right) & k^*\exp\left(-k\frac{a}{2}\right) \\ k^*\exp\left(k\frac{a}{2}\right) & -k\exp\left(-k^*\frac{a}{2}\right) \end{pmatrix} \begin{pmatrix} k\exp\left(k^*\frac{a}{2}\right) & k^*\exp\left(k\frac{a}{2}\right) \\ k^*\exp\left(-k\frac{a}{2}\right) & k\exp\left(-k^*\frac{a}{2}\right) \end{pmatrix}$$

[4]

This may be simplified as follows:

$$\Gamma_{single} = \frac{i}{2\,\mathrm{Im}[k]} \cdot \frac{1}{2\,\mathrm{Re}[k]} \begin{pmatrix} -k\exp\left(k^*\frac{a}{2}\right) & k^*\exp\left(-k\frac{a}{2}\right) \\ k^*\exp\left(k\frac{a}{2}\right) & -k\exp\left(-k^*\frac{a}{2}\right) \end{pmatrix} \begin{pmatrix} k\exp\left(k^*\frac{a}{2}\right) & k^*\exp\left(k\frac{a}{2}\right) \\ k^*\exp\left(-k\frac{a}{2}\right) & k\exp\left(-k^*\frac{a}{2}\right) \end{pmatrix}$$

$$= \frac{i}{4k_1k_2} \begin{pmatrix} -k^2\exp\left(k^*a\right)+\left(k^*\right)^2\exp\left(-ka\right) & -|k|^2\exp\left(k_2a\right)+|k|^2\exp\left(-k_2a\right) \\ |k|^2\exp\left(k_2a\right)-|k|^2\exp\left(-k_2a\right) & \left(k^*\right)^2\exp\left(ka\right)-\left(k\right)^2\exp\left(-k^*a\right) \end{pmatrix}$$

Here, we have used $kk^* = |k|^2$ (2 marks for seeing this). Remaining 4 marks to be awarded for the derivation of the matrix elements.

[6]

b) The determinant for Γ_{single} is derived as follows:

$$\det\left[\Gamma_{single}\right] = \left(\frac{i}{4k_1k_2}\right)^2 \left(\left(-k^2\exp\left(k^*a\right)+\left(k^*\right)^2\exp\left(-ka\right)\right)\left(\left(k^*\right)^2\exp\left(ka\right)-\left(k\right)^2\exp\left(-k^*a\right)\right)\right.$$
$$\left.-\left(|k|^2\exp\left(k_2a\right)-|k|^2\exp\left(-k_2a\right)\right)\left(-|k|^2\exp\left(k_2a\right)+|k|^2\exp\left(-k_2a\right)\right)\right)$$
$$= \left(\frac{i}{4k_1k_2}\right)^2 \left(-|k|^4\exp\left(2k_2a\right)+\left(k\right)^4+\left(k^*\right)^4-|k|^4\exp\left(-2k_2a\right)\right.$$
$$\left.+|k|^4\exp\left(2k_2a\right)-|k|^4-|k|^4+|k|^4\exp\left(-2k_2a\right)\right)$$
$$= \left(\frac{i}{4k_1k_2}\right)^2 \left(\left(k\right)^4+\left(k^*\right)^4-2|k|^4\right)$$

Here, the multiplying factor for T_{single} must not be left out (2 marks for seeing this). Remaining 6 marks to be awarded for the derivation of the expression above.

[8]

Hence, by using the expression given in the question, we find:

$$\det\left[\Gamma_{single}\right] = \left(\frac{i}{4k_1k_2}\right)^2 \left(\left(k\right)^4+\left(k^*\right)^4-2|k|^4\right) = \left(\frac{-1}{16k_1^2k_2^2}\right)\left(-16k_1^2k_2^2\right) = 1$$

[2]

c) To find the transmission coefficient for intensity T, for a wave incident only from the left hand side of the barrier, we can substitute $C = t$, the amplitude transmission coefficient, $D = 0$, no incident wave from the right, $A = 1$, and $B = r$, the amplitude reflection coefficient. We then have:

$$\begin{pmatrix} t \\ 0 \end{pmatrix} = T_{\text{single}} \begin{pmatrix} 1 \\ r \end{pmatrix} = \begin{pmatrix} T^{(1,1)} & T^{(1,2)} \\ T^{(2,1)} & T^{(2,2)} \end{pmatrix} \begin{pmatrix} 1 \\ r \end{pmatrix} = \begin{pmatrix} T^{(1,1)} + rT^{(1,2)} \\ T^{(2,1)} + rT^{(2,2)} \end{pmatrix}$$

$$\Rightarrow \begin{cases} t = \dfrac{T^{(1,1)}T^{(2,2)} - T^{(2,1)}T^{(1,2)}}{T^{(2,2)}} = \dfrac{1}{T^{(2,2)}} \\ r = -\dfrac{T^{(2,1)}}{T^{(2,2)}} \end{cases}$$

[4]

This gives the required expression for T:

$$T = |t|^2 = \left| \frac{1}{T^{(2,2)}} \right|^2 = \left(\frac{16k_1^2 k_2^2}{\left| \left(k^*\right)^2 \exp\left(ka\right) - \left(k\right)^2 \exp\left(-k^* a\right) \right|} \right)^2$$

[4]

Question 4 Answer

a) The designer chose a variable gap configuration because this gives higher sensitivity than variable overlap for the same nominal gap and overlap values. On the other hand, the variable overlap configuration offers better linearity. In the present device the displacements will be very small, so high sensitivity is the priority. Variable gap might be preferred in an application requiring linear transduction over larger displacements. [4]

b) The suspension stiffness is twice that of a single flexure i.e. $k = 24EI/L^3 = 2Ew^3h/L^3$. With E = 160 GPa, $w = 2.5$ μm, $h = 2$ μm and $L = 120$ μm, this gives k = **5.8 N/m**. [6]

The mass of the moving element is $\rho Ah = 2330 \times 0.05\times10^{-6} \times 2\times10^{-6} = 2.33\times10^{-10}$ kg. The resonance frequency is then obtained as $f_n = \frac{1}{2\pi}\sqrt{\frac{k}{m}}$ which gives f_n = **25.1 kHz**. [4]

b) According to parallel plate model, capacitance between adjacent electrode fingers is $\varepsilon_0 lh/g$, so total capacitance between terminal A and ground is $C_A \approx N_s \varepsilon_0 lh/g$ where N_s is the number of cells in the sensing section. With $N_s = 42$, $l = 100$ μm, $h = 2$ μm, $g = 1.3$ μm this gives $C_A \approx$ **57 fF**. [5]

The differential capacitance under applied acceleration is:

$$C_A - C_B = N_s \varepsilon_0 lh\left\{\frac{1}{g+x} - \frac{1}{g-x}\right\} \approx -\frac{2N_s\varepsilon_0 lh}{g^2}x = -2C_A\frac{x}{g}$$

where x is the displacement of mass relative to substrate (+ve displacement to right). For steady state acceleration a, the displacement is $x = -ma/k$.

With $m = 2.33\times10^{-10}$ kg and $k = 5.8$ N/m, the displacement at $a = 10$ ms^{-2} is $x = -0.40$ nm. The corresponding differential capacitance is $C_A - C_B \approx$ **0.035 fF**. [5]

d) Closure force for single parallel plate actuator (from memory / virtual work / force calc) is $\frac{1}{2}V^2\partial C/\partial g = -A\varepsilon_0 V^2/(2g^2)$. So, if a voltage V is applied between C and COM, the force acting on the proof mass (neglecting its small displacement) will be:

$$F = -\frac{N_a\varepsilon_0 lhV^2}{2g^2}$$

where N_a is the number of cells in the actuator. The equivalent acceleration would be $a = -F/m$. Combining these equations, and rearranging, the voltage required to emulate a given acceleration is:

$$V = \sqrt{\frac{2g^2 ma}{N_a\varepsilon_0 lh}}$$

With $N_a = 12$, and the other parameters as before, the voltage corresponding to $a = 10$ ms^{-2} is V = **0.6 V**. [6]

Question 5 Answer

a) Applying the method of sections to the flexure in Figure 5.1, the bending moment is:

$$M(x) = P(L-x) - F(v_L - v(x)) - C$$

where $v_L = v(L)$ is the end deflection. Taking moments for the overall structure gives $PL - Fv_L - 2C = 0$, and this allows the term in v_L to be eliminated, giving:

$$M(x) = -Px + Fv + C$$

The elementary bending equation is therefore:

$$EI\frac{d^2v}{dx^2} = -Px + Fv + C \quad \text{or} \quad \frac{d^2v}{dx^2} - \frac{F}{EI}v = \frac{C - Px}{EI} \qquad [6]$$

b) Using the c.f./p.i. method, the general solution for the bending equation is:

$$v = A\cosh(\kappa x) + B\sinh(\kappa x) + \frac{Px - C}{F} \qquad [4]$$

The boundary conditions $v = 0$ and $v' = 0$ at $x = 0$ give $A = C/F$ and $B = -P/\kappa F$ respectively. The boundary condition $v' = 0$ at $x = L$ gives $C = P(\cosh \kappa L - 1)/(\kappa \sinh \kappa L)$. With these values for A, B and C, the end deflection is obtained as:

$$v_L = \frac{P}{kF}\left[\frac{(\cosh \kappa L - 1)^2}{\sinh \kappa L} + \kappa L - \sinh \kappa L\right]$$

and the stiffness is :

$$k = \frac{P}{v_L} = \frac{F}{L}\frac{\kappa L \sinh \kappa L}{(\cosh \kappa L - 1)^2 + \kappa L \sinh \kappa L - \sinh^2 kL}. \qquad [4]$$

With the application of the identity $\cosh^2 x - \sinh^2 x = 1$, this reduces to:

$$k = \frac{P}{v_L} = \frac{F}{L}\frac{\kappa L \sinh \kappa L}{2(1 - \cosh \kappa L) + \kappa L \sinh \kappa L} \qquad [2]$$

The required approximate form is obtained by replacing the hyperbolic functions with series expansions. Terms up to 6th order need to be included in the denominator. [4]

c) Consider the effect of a temperature change ΔT on the flexures at either the top or bottom of the suspension. The span (from LH end left flexure to RH end of right flexure) is $(2L + g)$ before the temperature change, where L is the flexure length. The change in span under unconstrained expansion would be $(2L\alpha_m + g\alpha_s)\Delta T$, where α_m and α_s are the CTEs of nickel and silicon respectively. However, the proof mass constrains the expansion, forcing the change in length to be $(2L + g)\alpha_m \Delta T$. The resulting thermal strain in the flexures is the difference between these two, divided by $2L$:

$$\varepsilon_{th} = (\alpha_m - \alpha_s) g \Delta T / 2L \qquad [4]$$

Since $\alpha_m > \alpha_s$, an increase in temperature causes tensile strain which will increase the stiffness. The effect therefore has the correct sign to provide compensation for the decreasing Young's modulus, and we just need to choose g to give the required level of compensation.

The thermal strain gives rise to an axial load of $F = Ewh\varepsilon_{th}$, where w and h are the flexure width and depth, and the resulting factional change in stiffness is:

$$\frac{\delta k}{k} = \frac{FL^2}{10EI} = \frac{12wh\varepsilon_{th}L^2}{10Ew^3h} = \frac{6L^2\varepsilon_{th}}{5w^2}$$

Combining this with the previous equation gives:

$$\frac{\delta k}{k} = \frac{3}{5}\frac{gL}{w^2}(\alpha_m - \alpha_s)\Delta T \qquad [4]$$

To compensate for the change in Young's modulus, we require $\delta k/k = 0.0286$ % when $\Delta T = 1$ °C. With these values and with $(\alpha_m - \alpha_s) = 10.8 \times 10^{-6}$ K^{-1}, $w = 10$ μm, $L = 200$ μm, the above equation gives $g = \mathbf{22}$ **μm**. [2]